

# Analysis of Shadow Moire Technique With Phase Shifting Using Generalisation of Carre Method

P. A. A. Magalhaes Jr\*, P. S. Neto\* and C. S. de Barcellos†

\*Pontificia Universidade Catolica de Minas Gerais - Av. Dom Jose Gaspar 500, 30535-610, Belo Horizonte, Minas Gerais, Brasil, Brazil

†Universidade Federal de Santa Catarina, Florianopolis, Santa Catarina, Brasil, Brazil

**ABSTRACT:** Experimental stress analysis can be conveniently investigated by classical shadow Moire technique. Moire is a non-contact and non-destructive technique, with a fast digitisation process. The phenomena of Moire fringes are the result of the projection of the fringes of a ruling on a certain object. It has measurement accuracy comparable with other systems and also low cost. The present study offers new algorithms for phase evaluation in measurements. Several phase-shifting algorithms with an arbitrary but constant phase-shift between captured intensity signs are proposed. The algorithms are similarly derived as the so-called 'Carre algorithm'. The idea is to develop a generalisation of Carre algorithm that is not restricted to four images. Errors and random noise in the images cannot be eliminated, but the uncertainty caused by their effects can be reduced by increasing the number of observations. An experimental analysis of the mistakes of the technique was made, as well as a detailed analysis of mistakes of the measurement. The advantages of the proposed algorithm are its precision in the measures taken, speed of processing and the immunity to noise in signs and images.

**KEY WORDS:** *Carre algorithm, experimental strain analysis, experimental stress analysis, measurement, phase calculation algorithms, phase-shifting technique*

## Introduction

Phase shifting is an important technique in experimental strain analysis [1–3]. Conventional phase-shifting algorithms require phase-shift amounts to be known; however, errors on phase shifts are common for the phase-shift modulators in real applications, and such errors can further cause substantial errors in the determination of phase distributions. There are many potential error sources which may affect the accuracy of the practical measurement, e.g. phase-shifting errors, detector nonlinearities, quantisation errors, source stability, vibrations and air turbulence [4].

Currently, the phase-shifting technique is the most widely used technique for evaluation of interference fields in many areas of science and engineering. Its principle is based on the evaluation of the phase values from several phase-modulated measurements of the intensity of the interference field. It is necessary to carry out at least three phase-shifted intensity measurements to determine unambiguously and very accurately, the phase at every point of the detector plane. The phase-shifting technique offers a fully automatic calculation of the phase difference between two coherent wave fields that interfere in the process. There are various phase-shifting algorithms for phase

calculation that differ on the number of phase steps, on phase-shift values between captured intensity frames and on their sensitivity to the influencing factors during practical measurements [4].

The general principle of most interferometric measurements is as follows. Two light beams (reference and object) interfere after an interaction of the object beam with the measured object, i.e. the beam is transmitted or reflected by the object. The distribution of the intensity of the interference field is then detected, using a photographic film, charge-coupled device (CCD) camera, etc. The phase difference between the reference and the object beam can be determined using the above-mentioned phase calculation techniques. The phase-shifting technique is based on an evaluation of the phase of the interference signal using phase modulation of this interference signal [5].

## Theory of the Phase-Shifting Technique

The fringe pattern is assumed to be a sinusoidal function and is represented by the intensity distribution  $I(x,y)$ . This function can be written in general form as:

$$I(x, y) = I_m(x, y) + I_a(x, y) \cos[\phi(x, y) + \delta] \tag{1}$$

where  $I_m$  is the background intensity variation,  $I_a$  is the modulation strength,  $\phi(x, y)$  is the phase at origin and  $\delta$  is the phase shift related to the origin [6].

The general theory of synchronous detection can be applied to discrete sampling procedure, with only a few sample points. There must be at least four signal measurements to determine the phase  $\phi$  and the term  $\delta$ . Phase shifting is the preferred technique whenever the external turbulence and mechanical conditions of the images remain constant over the time required to obtain the four phase-shifted frames. The technique used in this experiment is called the ‘Carre method’ [7]. By solving the Equation (1) above, the phase  $\phi$  can be determined. The intensity distribution of fringe pattern in a pixel may be represented by grey level, which varies from 0 to 255. With the Carre method, the phase shift ( $\delta$ ) amount is treated as an unknown value. The method uses four phase-shifted images as

$$\begin{cases} I_1(x, y) = I_m(x, y) + I_a(x, y) \cos[\phi(x, y) - 3\delta/2] \\ I_2(x, y) = I_m(x, y) + I_a(x, y) \cos[\phi(x, y) - \delta/2] \\ I_3(x, y) = I_m(x, y) + I_a(x, y) \cos[\phi(x, y) + \delta/2] \\ I_4(x, y) = I_m(x, y) + I_a(x, y) \cos[\phi(x, y) + 3\delta/2] \end{cases} \tag{2}$$

Assuming that the phase shift is linear and does not change during the measurements, the phase at each point is determined as

$$\phi = \arctan \left\{ \frac{\sqrt{[(I_1 - I_4) + (I_2 - I_3)][3(I_2 - I_3) - (I_1 - I_4)]}}{(I_2 + I_3) - (I_1 + I_4)} \right\} \tag{3}$$

Expanding Equation (3), we obtain the Carre method as:

$$\tan(\phi) = \frac{\sqrt{\begin{vmatrix} -I_1^2 & +2I_1I_2 & -2I_1I_3 & +2I_1I_4 \\ & +3I_2^2 & -6I_2I_3 & -2I_2I_4 \\ & & +3I_3^2 & +2I_3I_4 \\ & & & -I_4^2 \end{vmatrix}}}{|-I_1 + I_2 + I_3 - I_4|} \tag{4}$$

or emphasising only the matrix of coefficients of the numerator and the denominator:

$$\tan(\phi) = \frac{\sqrt{|\text{Num}|}}{|\text{Dem}|} \quad \text{Num} = \begin{bmatrix} -1 & 2 & -2 & 2 \\ & 3 & -6 & -2 \\ & & 3 & 2 \\ & & & -1 \end{bmatrix} \tag{5}$$

$$\text{Dem} = [-1 \quad 1 \quad 1 \quad -1]$$

Almost all the existing phase-shifting algorithms are based on the assumption that the phase-shift at all pixels of the intensity frame is equal and known. However, it may be very difficult to achieve this in practice. Phase-measuring algorithms are more or less sensitive to some types of errors that can occur during measurements with images. The phase-shift value is assumed unknown but is constant in phase calculation algorithms, which are derived in this paper. Consider now the constant but unknown phase-shift value  $\delta$  between recorded images of the intensity of the observed interference field.

Considering  $N$  phase-shifted intensity measurements, we can write for the intensity distribution  $I_k$  at every point of  $k$  recorded phase-shifted interference patterns.

$$I_k(x, y) = I_m(x, y) + I_a(x, y) \cos \left[ \phi(x, y) + \left( \frac{2k - N - 1}{2} \right) \delta \right] \tag{6}$$

where  $k = 1, \dots, N$  and  $N$  being the number of frames.

In Novak [4], several five-step phase-shifting algorithms insensitive to phase-shift calibration are described, and a complex error analysis of these phase calculation algorithms is performed. The best five-step algorithm, Equation (7), seems to be a very accurate and stable phase-shifting algorithm with the unknown phase step for a wide range of phase-step values.

$$\begin{cases} a_{jk} = I_j - I_k \\ b_{jk} = I_j + I_k \end{cases} \quad \tan(\phi) = \frac{\sqrt{4a_{24}^2 - a_{15}^2}}{2I_3 - b_{15}} = \frac{\sqrt{4(I_2 - I_4)^2 - (I_1 - I_5)^2}}{2I_3 - I_1 - I_5} \tag{7}$$

Expanding Equation (7), we obtain the Novak method as:

$$\tan(\phi) = \frac{\sqrt{\begin{vmatrix} -I_1^2 & & & +2I_1I_5 \\ & +4I_2^2 & -8I_2I_4 & \\ & & +4I_4^2 & \\ & & & -I_5^2 \end{vmatrix}}}{|-I_1 + 2I_3 - I_5|} \tag{8}$$

or emphasising only the matrix of coefficients of the numerator and the denominator:

$$\tan(\phi) = \frac{\sqrt{|\text{Num}|}}{|\text{Dem}|} \quad \text{Num} = \begin{bmatrix} -1 & 0 & 0 & 0 & 2 \\ & 4 & 0 & -8 & 0 \\ & & 0 & 0 & 0 \\ & & & 4 & 0 \\ & & & & -1 \end{bmatrix}$$

$$\text{Dem} = [-1 \quad 0 \quad 2 \quad 0 \quad -1] \tag{9}$$

### Proposed Algorithms

A general algorithm for calculating the phase for any number,  $N$ , of images  $\tan(\phi) = \text{Sqrt}(\text{Abs}(\text{Num})/\text{Abs}(\text{Dem}))$  is proposed here:

$$\tan(\phi) = \frac{\sqrt{|\text{Num}|}}{|\text{Dem}|} = \frac{\sqrt{\left| \sum_{r=1}^N \sum_{s=r}^N n_{r,s} I_r I_s \right|}}{\left| \sum_{r=1}^N d_r I_r \right|} \tag{10}$$

where  $N$  is the number of images,  $n_{r,s}$  are coefficients of the numerator (Num),  $d_r$  are coefficients of the denominator (Dem), and  $r$  and  $s$  are indexes of the sum. Or, expanding the summations and allowing an arbitrary number of lines

$$\tan(\phi) = \frac{\sqrt{\begin{matrix} n_{1,1}I_1^2 & +n_{1,2}I_1I_2 & +n_{1,3}I_1I_3 & +n_{1,4}I_1I_4 & \cdots & +n_{1,N}I_1I_N \\ & +n_{2,2}I_2^2 & +n_{2,3}I_2I_3 & +n_{2,4}I_2I_4 & \cdots & +n_{2,N}I_2I_N \\ & & +n_{3,3}I_3^2 & +n_{3,4}I_3I_4 & \cdots & +n_{3,N}I_3I_N \\ & & & +n_{4,4}I_4^2 & \cdots & +n_{4,N}I_4I_N \\ & & & & \cdots & \cdots \\ & & & & & +n_{N,N}I_N^2 \end{matrix}}{|d_1I_1 + d_2I_2 + d_3I_3 + d_4I_4 + \cdots + d_{N-1}I_{N-1} + d_NI_N|} \tag{11}$$

Or, emphasising only the matrix of coefficients of the numerator and the denominator:

$$\tan(\phi) = \frac{\sqrt{|\text{Num}|}}{|\text{Dem}|} \left\{ \begin{array}{l} \text{Num} = \begin{bmatrix} n_{1,1} & n_{1,2} & n_{1,3} & n_{1,4} & \cdots & n_{1,N} \\ & n_{2,2} & n_{2,3} & n_{2,4} & \cdots & n_{2,N} \\ & & n_{3,3} & n_{3,4} & \cdots & n_{3,N} \\ & & & n_{4,4} & \cdots & n_{4,N} \\ & & & & \cdots & \cdots \\ & & & & & n_{N,N} \end{bmatrix} \\ \text{Dem} = [d_1 \ d_2 \ d_3 \ d_4 \ \cdots \ d_{N-1} \ d_N] \end{array} \right. \tag{12}$$

The display of the phase calculation algorithm in this way permits the viewing of symmetries and plans of sparse matrix. The use of the absolute value in the numerator and the denominator restricts the angle between  $0^\circ$  and  $90^\circ$  but avoids negative roots, and also eliminates false angles found. Subsequent considerations will later remove this restriction [4–6].

In the tested practical applications, an increase in 20% in the processing time was noticed when using 16 images instead of four while processing the standard Carre algorithm, because of many zero coefficients. But if one changes the coefficients from integer type to real numbers, the processing time for the evaluation of phase practically doubles because real numbers use more memory and more processing

time to evaluate floating point additions and multiplications, which are many in the algorithms with a large quantity of images.

The shift on the problem focus of obtaining algorithms for calculating the phase of an analytical problem of a numerical vision is a great innovation. It breaks a paradigm that was hitherto used by several authors. After several attempts in numerical modeling of the problem, the following mathematical problem was identified:

$$\begin{array}{l} \text{Minimal } \sum_{r=1}^N \sum_{s=r}^N |n_{r,s}| + \sum_{r=1}^N |d_r| \\ \text{subject } \left\{ \begin{array}{ll} \tan(\phi) = \text{Sqrt}(|\text{Num}|)/|\text{Dem}| & \text{number of variables} \\ \text{(i) } \tan^2(\phi^v) \left( \sum_{r=1}^N d_r I_r^v \right)^2 = \sum_{r=1}^N \sum_{s=r}^N n_{r,s} I_r^v I_s^v, & v = 1, \dots, \left[ \frac{(N+1)N}{2} + N \right] \\ \text{(ii) } \sum_{s=r}^N |n_{r,s}| + |d_r| \geq 1, & r = 1, \dots, N, \text{ enter all frames} \\ \text{(iii) } \sum_{s=r}^N |n_{s,r}| + |d_r| \geq 1, & r = 1, \dots, N, \text{ enter all frames} \\ \text{(iv) } -2N \leq n_{r,s} \leq 2N, & r = 1, \dots, N, \ s = r, \dots, N \\ \text{(v) } -2N \leq d_s \leq 2N, & r = 1, \dots, N \\ \text{(vi) } n_{r,s} \text{ are integer,} & r = 1, \dots, N, \ s = r, \dots, N \\ \text{(vii) } d_r \text{ are integer,} & r = 1, \dots, N \end{array} \right. \end{array}$$

where for each  $v$ :

$$\begin{cases} I_k^v(x, y) = I_m^v(x, y) + I_a^v(x, y) \cos[\phi^v(x, y) + (\frac{2k-N-1}{2})\delta^v], & k = 1, \dots, N \\ I_m^v \in [0; 128] & \text{random and real} \\ I_a^v \in [0; 127] & \text{random and real} \\ \phi^v \in [-\pi; \pi] & \text{random and real} \\ \delta^v \in [-2\pi; 2\pi] & \text{random and real} \end{cases} \tag{13}$$

The coefficients of the matrices of the numerator ( $n_{r,s}$ ) and the denominator ( $d_r$ ) must be integers to increase the performance of the computer algorithm, as the values of the intensity of the images ( $I_k$ ) are also integers ranging from 0 to 255. Modern computers perform integer computations (additions and multiplications) much faster than floating-point computations. It should be noted that currently the commercial digital photographic cameras present graphics resolution above 12 megapixels and that the evaluation of phase ( $\phi$ ) should be done pixel to pixel. Another motivation is the use of memory: integer values can be stored on a single byte while real values use, at least, 4 bytes. The present scheme uses real numbers only in the square root of the numerator, in the division by denominator and in the arc-tangent over the entire operation.

The idea of obtaining a minimum sum of the values of absolute or module of the coefficients of matrices of the numerator ( $n_{r,s}$ ) and denominator ( $d_r$ ) comes from the attempt to force these factors to zero, for computational speed up and for reducing the required memory, as zero terms in sparse matrices do not need to be stored. It is also important that those ratios are not very large so that the sum of the numerator and the denominator do not have very high value to fit into an integer variable. For a precise phase evaluation, these factors will increase the values of the intensity of the image ( $I_k$ ) that contains errors because of noise in the image, in its discretisation in pixels and in shades of grey.

The first restriction of the problem (13) is the Equation (10), which is squared to form the relation that one is seeking. Note that the results obtained by solving the mathematical problem of the coefficients are in the form of matrices for the numerator ( $n_{r,s}$ ) and the denominator ( $d_r$ ), so the number of unknowns is given by  $v$ . To ensure that one has a hyper-restricted problem, the number of restrictions must be greater than or at least equal to the number of variables. The  $v$  restrictions of the model are obtained through random choice of values for  $I_m$ ,  $I_a$ ,  $\phi$  and  $\delta$  and by using the Equation (6) to compute  $I_k$ . Tests showed that even for low numbers for other

values of  $v$ , the mathematical problem leads to only one optimal solution though it becomes more time

consuming. Indeed the values of  $I_m$ ,  $I_a$ ,  $\phi$  and  $\delta$  can be any real number, but to maintain compatibility with the problem images, it was decided to limit  $I_m$  between 0 to 128 and  $I_a$  between 0 and 127 so that  $I_k$  would be between 0 and 255.

The restrictions (ii) and (iii) of the problem are based on the idea that all image luminous intensities,  $I_k$ , must be present in the algorithm. It increases the amounts of samples to reduce the noise of random images. This requires that all the sampling images enter the algorithm for phase calculation. This is achieved by imposing that the sum of the absolute values of the coefficients of each row or column of the matrix of each of the numerator ( $n_{r,s}$ ), plus the module at the rate corresponding to that image in the denominator ( $d_r$ ), is greater than or equal to 1. Thus the coefficients on an algorithm to calculate the phase for a given image  $I_k$  will not be all zeros, ensuring their participation in the algorithm.

Restrictions (iv) and (v) of the problem are used to accelerate the solution of this mathematical model. This limitation in the value of the coefficients of matrices of the numerator ( $n_{r,s}$ ) and denominator ( $d_r$ ) presents a significant reduction in the search universe and in the search of a solution for model optimisation. Whenever  $N$  is greater than 16, the coefficients of matrices of the numerator ( $n_{r,s}$ ) and denominator ( $d_r$ ) can be limited to the interval  $[-4,4]$ . The search is restricted to coefficients of matrices of the numerator ( $n_{r,s}$ ) and denominator ( $d_r$ ), which are integers of small value and meeting the restrictions of the model; it does not need to be minimised (desirable but not necessary).

Once a solution to the problem is found, it can become a restriction. Therefore, solving the problem again leads to a different solution. This allows the problem (13) to lead to many different algorithms for a given value of  $N$ , making it very flexible and the numerical problem, comprehensive. The following multi-step algorithm for phase calculation uses well-known trigonometric relations and branch-and-bound algorithm [8] for pure integer nonlinear programming with the mathematic problem (13). Tables 1 to 3 show some algorithms.

**Table 1:** Matrix of coefficient for  $N = 4$  and  $N = 5$ , with type  $\tan(\phi) = \text{Sqrt}(|\text{Num}|)/|\text{Dem}|$

N = 4	Num	-1	2	-2	2	
	a)		3	-6	-2	
				3		2
Dem	-1	1	1	-1		
N = 5	Num	-1	0	0	0	2
	a)		4	0	-8	0
				0	0	0
Dem	-1	0	2	0	-1	-1

Following the model of uncertainty analysis presented in Refs [4, 9], these new algorithms have excellent results with the application of the Monte Carlo-based technique of uncertainty propagation. The Monte Carlo-based technique requires assigning probability density functions (PDFs) to each input quantity. A computer algorithm is set up to generate an input vector  $P = (p_1 \dots p_n)^T$ ; each element  $p_j$  of this vector is generated according to the specific PDF assigned to the corresponding quantity  $p_j$ . By applying the generated vector  $P$  to the model  $Q = M(P)$ , the corresponding output value  $Q$  can be computed. If the simulating process is repeated  $n$  times ( $n \gg 1$ ), the outcome is a series of indications  $(q_1, \dots, q_n)$ , the frequency distribution of which allows us to identify the PDF of  $Q$ . Then, irrespective of the form of this PDF, the estimate  $q_e$  and its associated standard uncertainty  $u(q_e)$  can be calculated by

$$q_e = \frac{1}{n} \sum_{l=1}^n q_l, \tag{14}$$

and

$$u(q_e) = \sqrt{\frac{1}{(n-1)} \sum_{l=1}^n (q_l - q_e)^2}. \tag{15}$$

The influence of the error sources affecting the phase values is considered in these models through the values of the intensity  $I_k$ . This is done by modifying Equation (6):

$$I_k(x, y) = I_m(x, y) + I_a(x, y) \cos \left[ \phi(x, y) + \left( \frac{2k - N - 1}{2} \right) (\delta + \theta) + \varepsilon_k \right] + \xi_k. \tag{16}$$

$$\begin{cases} d_r = d_{N+1-r}, & r = 1, \dots, h \text{ and } r \neq N + 1 - r \\ n_{r,N+1-r} = -2n_{r,r}, & r = 1, \dots, h \text{ and } r \neq N + 1 - r \\ n_{N+1-s,N+1-r} = n_{r,s}, & r = 1, \dots, h; s = r, \dots, h \text{ and } r \neq N + 1 - s \text{ and } s \neq N + 1 - r \\ n_{r,N+1-s} = -n_{r,s}, & r = 1, \dots, h; s = r, \dots, h \text{ and } s > r \text{ and } s \neq N + 1 - s \\ n_{s,N+1-r} = -n_{r,s}, & r = 1, \dots, h; s = r, \dots, h \text{ and } s > r \text{ and } s \neq N + 1 - r \end{cases} \tag{17}$$

Comparing Equations (6) and (16), it can be observed that three input quantities ( $\theta, \varepsilon_k, \xi_k$ ) were included.  $\theta$  allows us to consider, in the uncertainty propagation, that the systematic error used to induce the phase shift is not adequately calibrated. The error bound allowed us to assign to  $\theta$  a rectangular PDF over the interval  $(-\pi/10 \text{ rad}, +\pi/10 \text{ rad})$ .  $\varepsilon_k$  allowed us to account for the influence of environmental perturbations. The error bound allowed us to assign to  $\varepsilon_k$  a rectangular PDF over the interval  $(-\pi/20 \text{ rad}, +\pi/20 \text{ rad})$ .  $\xi_k$  allows us to account for the nearly random effect of the optical noise. The rectangular PDFs assigned to  $\xi_k$  should be in the interval  $(-10, +10)$ .

The values of  $\phi$  were considered given in the range  $(0, \pi/2)$ . A computer algorithm was set up to generate single values of  $(\theta, \varepsilon_k, \xi_k)$  according to the corresponding PDFs. With the generated values of the input quantities, we evaluated the phase  $\phi'$  by using the new algorithms. As this simulating process and the corresponding phase evaluation were repeated  $n = 10^4 = 10\,000$  times, we were able to form the series  $(\phi'_1 \dots \phi'_{10000})$  with the outcomes.

The algorithms with letters (a) are better, more accurate, more robust and more stable for the random noise. The tests show that the optimum phase-shift interval with which the algorithm gives minimum uncertainty for the noise is in the vicinity of  $\pi/2$  radians (Figure 1).

Figure 2 shows the average of the standard uncertainty  $u(\phi')$  generated with values  $\phi$  in the range  $(0, \pi/2)$  by using new algorithms. It can be observed that the uncertainty by new algorithms diminishes as the number of images increases.

### Symmetry and Sparse in Matrix of Coefficient

Solving the problem of increasing the processing time to obtain new formulas for phase calculation with the increased number of variables for high values of  $N$  uses up important data; most of the formulas showed symmetries in the matrix of coefficients of the numerator and the denominator. Let  $h = (N \text{ div } 2) + (N \text{ mod } 2)$  where the value of  $x \text{ div } y$  is the value of  $x/y$  rounded in the direction of zero to the nearest integer (integer division) and the mod operator returns the remainder obtained by dividing its operands [in other words,  $x \text{ mod } y = x - (x \text{ div } y) * y$ ]. The symmetries are:

**Table 2:** Matrix of coefficient for  $N = 6, \dots, 12$ , with type  $\tan(\phi) = \text{Sqrt}(|\text{Num}|)/|\text{Dem}|$

N = 6	Num	-1	0	-1	1	0	2													
	a)		3	1	-1	-6	1													
	Dem	-1	0	1	1	0	-1													
N = 7	Num	-1	-2	-3	0	3	2	2												
	a)		4	6	2	0	-6	-8												
	Dem	-1	-1	1	2	1	-1													
N = 8	Num	-1	0	1	0	0	-1	0	2											
	a)		1	0	-2	2	0	-2	0											
	Dem	-1	0	1	0	0	1	0	-1											
N = 9	Num	-1	2	-1	0	0	0	1	-2	2										
	a)		0	-2	6	0	0	-12	2	1										
	Dem	-1	1	0	-1	2	-1	0	1	-1										
N = 10	Num	-1	0	1	0	0	0	0	-1	2										
	a)		1	0	-1	0	0	1	0	-2										
	Dem	-1	0	1	0	0	0	0	1	-1										
N = 11	Num	-1	0	-1	-2	0	0	0	2	1	0	2								
	a)		1	0	2	0	0	-2	0	-2	0	1								
	Dem	-1	0	0	-1	1	2	1	-1	0	0	-1								
N = 12	Num	-1	0	1	0	0	0	0	0	-1	0	2								
	a)		1	0	-1	0	0	0	0	1	0	0								
	Dem	-1	0	1	0	0	0	0	0	1	0	-1								



So as the matrix for  $N$  also was:

$$\text{Num} = \begin{bmatrix} n_{1,1} & n_{1,2} & n_{1,3} & \cdots & n_{1,h-1} & n_{1,h} & -n_{1,h} & -n_{1,h-1} & \cdots & -n_{1,3} & -n_{1,2} & -2n_{1,1} \\ & n_{2,2} & n_{2,3} & \cdots & n_{2,h-1} & n_{2,h} & -n_{2,h} & -n_{2,h-1} & \cdots & -n_{2,3} & -2n_{2,2} & -n_{1,2} \\ & & n_{3,3} & \cdots & n_{3,h-1} & n_{3,h} & -n_{3,h} & -n_{3,h-1} & \cdots & -2n_{3,3} & -n_{2,3} & -n_{1,3} \\ & & & \cdots & \cdots & \cdots & \cdots & \cdots & \cdots & \cdots & \cdots & \cdots \\ & & & & n_{h-1,h-1} & n_{h-1,h} & -n_{h-1,h} & -2n_{h-1,h-1} & \cdots & -n_{3,h-1} & -n_{2,h-1} & -n_{1,h-1} \\ & & & & & n_{h,h} & -2n_{h,h} & -n_{h-1,h} & \cdots & -n_{3,h} & -n_{2,h} & -n_{1,h} \\ & & & & & & n_{h,h} & n_{h-1,h} & \cdots & n_{3,h} & n_{2,h} & n_{1,h} \\ & & & & & & & n_{h-1,h-1} & \cdots & n_{3,h-1} & n_{2,h-1} & n_{1,h-1} \\ & & & & & & & & \cdots & \cdots & \cdots & \cdots \\ & & & & & & & & & n_{3,3} & n_{2,3} & n_{1,3} \\ & & & & & & & & & & n_{2,2} & n_{1,2} \\ & & & & & & & & & & & n_{1,1} \end{bmatrix} \tag{18}$$

$$\text{Dem} = [d_1 \ d_2 \ d_3 \ d_4 \ \cdots \ d_{h-1} \ d_h \ d_h \ d_{h-1} \ \cdots \ d_4 \ d_3 \ d_2 \ d_1]$$

In addition, the matrix for odd  $N$  was:

$$\text{Num} = \begin{bmatrix} n_{1,1} & n_{1,2} & n_{1,3} & \cdots & n_{1,h-1} & n_{1,h} & -n_{1,h-1} & \cdots & -n_{1,3} & -n_{1,2} & -2n_{1,1} \\ & n_{2,2} & n_{2,3} & \cdots & n_{2,h-1} & n_{2,h} & -n_{2,h-1} & \cdots & -n_{2,3} & -2n_{2,2} & -n_{1,2} \\ & & n_{3,3} & \cdots & n_{3,h-1} & n_{3,h} & -n_{3,h-1} & \cdots & -2n_{3,3} & -n_{2,3} & -n_{1,3} \\ & & & \cdots & \cdots & \cdots & \cdots & \cdots & \cdots & \cdots & \cdots \\ & & & & n_{h-1,h-1} & n_{h-1,h} & -2n_{h-1,h-1} & \cdots & -n_{3,h-1} & -n_{2,h-1} & -n_{1,h-1} \\ & & & & & n_{h,h} & n_{h-1,h} & \cdots & n_{3,h} & n_{2,h} & n_{1,h} \\ & & & & & & n_{h-1,h-1} & \cdots & n_{3,h-1} & n_{2,h-1} & n_{1,h-1} \\ & & & & & & & \cdots & \cdots & \cdots & \cdots \\ & & & & & & & & n_{3,3} & n_{2,3} & n_{1,3} \\ & & & & & & & & & n_{2,2} & n_{1,2} \\ & & & & & & & & & & n_{1,1} \end{bmatrix} \tag{19}$$

$$\text{Dem} = [d_1 \ d_2 \ d_3 \ d_4 \ \cdots \ d_{h-1} \ d_h \ d_{h-1} \ \cdots \ d_4 \ d_3 \ d_2 \ d_1]$$

Therefore, using symmetry to the numerator coefficients can be represented with only its first quarter and the denominator coefficients can be represented only with the first half, as shown below:

numerator, the terms are different from zero in the main diagonal and closer to the three diagonal, so only the first four coefficients of each line are different from zero. In the first half of the coefficients of

$$\text{Num}^{1/4} = \begin{bmatrix} n_{1,1} & n_{1,2} & n_{1,3} & \cdots & n_{1,h-1} & n_{1,h} \\ & n_{2,2} & n_{2,3} & \cdots & n_{2,h-1} & n_{2,h} \\ & & n_{3,3} & \cdots & n_{3,h-1} & n_{3,h} \\ & & & \cdots & \cdots & \cdots \\ & & & & n_{h-1,h-1} & n_{h-1,h} \\ & & & & & n_{h,h} \end{bmatrix} \quad \text{Dem}^{1/2} = [d_1 \ d_2 \ d_3 \ \cdots \ d_{h-1} \ d_h] \tag{20}$$

In previous formulas, most of the coefficients of the numerator and the denominator are zero. Even more for the first quarter of the coefficients of the

the denominator, only the first four and the last term are different from zero. A matrix where most of the terms are zeros is usually called sparse matrix.

$$\text{Sparse} \begin{cases} d_r^{1/2} = 0, & r = 5, \dots, h-1 \\ n_{r,s}^{1/4} = 0, & r = 1, \dots, h-5, \quad s = r+4, \dots, h, \text{ and } s > r+3 \end{cases} \tag{21}$$







For case 4, when  $N$  is even,  $N + 2$  is divisible by 4  
but  $N + 2$  is not divisible by 8:

Half =  $N/2$

Fourth =  $(N + 2)/4$

$$\begin{array}{l}
 \text{Num}^{1/4} = \left[ \begin{array}{cccccccc}
 -1 & 0 & 1 & 0 & \dots & & & \\
 & 1 & 0 & -1 & 0 & \dots & & \\
 & & 0 & 0 & 1 & 0 & \dots & \\
 & & & -1 & 0 & 0 & 0 & \dots \\
 & & & & 0 & 0 & 1 & 0 & \dots \\
 & & & & & -1 & 0 & 0 & 0 & \dots \\
 & & & & & & \dots & \dots & \dots & \dots \\
 & & & & & & & 0 & 0 & -1 & 0 & \dots \\
 & & & & & & & & 1 & 0 & 0 & 0 & \dots \\
 & & & & & & & & & 0 & 0 & -1 & 0 & \dots \\
 & & & & & & & & & & 1 & 0 & 0 & 0 & \dots \\
 & & & & & & & & & & \dots & \dots & \dots & \dots & \dots \\
 & & & & & & & & & & & 1 & 0 & -1 & 0 \\
 & & & & & & & & & & & & 1 & 0 & 0 \\
 & & & & & & & & & & & & & 0 & 1 \\
 & & & & & & & & & & & & & & 1
 \end{array} \right]
 \end{array}
 \begin{array}{l}
 \text{Row :} \\
 1 \\
 2 \\
 3 \\
 4 \\
 \text{Repeat} \\
 \text{Repeat} \\
 \dots \\
 \text{Fourth} \\
 \text{Fourth} + 1 \\
 \text{Repeat} \\
 \text{Repeat} \\
 \dots \\
 \text{Half} - 3 \\
 \text{Half} - 2 \\
 \text{Half} - 1 \\
 \text{Half}
 \end{array}
 \tag{26}$$

$$\begin{array}{l}
 \text{Dem}^{1/2} = [-1 \ 0 \ 1 \ 0 \ 0 \ 0 \ \dots \quad 0 \quad 0 \quad 0] \\
 \text{Col} \quad : 1 \ 2 \ 3 \ 4 \ 5 \ 6 \ \dots \quad \text{Half} - 2 \quad \text{Half} - 1 \quad \text{Half}
 \end{array}$$

For case 5, when  $N$  is odd,  $N - 1$  is divisible by 4  
and  $N - 1$  is divisible by 8:

Half =  $(N + 1)/2$

Fourth =  $(N - 1)/4$

$$\begin{array}{l}
 \text{Num}^{1/4} = \left[ \begin{array}{cccccccc}
 -1 & 2 & -1 & 0 & \dots & & & \\
 & 0 & -2 & 0 & 0 & \dots & & \\
 & & 2 & 0 & -1 & 0 & \dots & \\
 & & & 0 & 0 & 0 & 1 & \dots \\
 & & & & 0 & -1 & 0 & 0 & \dots \\
 & & & & & \dots & \dots & \dots & \dots \\
 & & & & & & 0 & 0 & 2 & -2 & \dots \\
 & & & & & & & 2 & -2 & 0 & 2 & \dots \\
 & & & & & & & & 0 & 2 & 0 & 0 & \dots \\
 & & & & & & & & & 0 & 0 & 0 & -1 & \dots \\
 & & & & & & & & & & 0 & 1 & 0 & 0 & \dots \\
 & & & & & & & & & & \dots & \dots & \dots & \dots & \dots \\
 & & & & & & & & & & & 0 & -2 & 0 \\
 & & & & & & & & & & & & 2 & 0 \\
 & & & & & & & & & & & & & 0
 \end{array} \right]
 \end{array}
 \begin{array}{l}
 \text{Row :} \\
 1 \\
 2 \\
 3 \\
 \text{Repeat} \\
 \text{Repeat} \\
 \dots \\
 \text{Fourth} \\
 \text{Fourth} + 1 \\
 \text{Fourth} + 2 \\
 \text{Repeat} \\
 \text{Repeat} \\
 \dots \\
 \dots \\
 \text{Half} - 2 \\
 \text{Half} - 1 \\
 \text{Half}
 \end{array}
 \tag{27}$$

$$\begin{array}{l}
 \text{Dem}^{1/2} = [-1 \ 1 \ 0 \ -1 \ 0 \ 0 \ \dots \quad 0 \quad 0 \quad 2] \\
 \text{Col} \quad : 1 \ 2 \ 3 \ 4 \ 5 \ 6 \ \dots \quad \text{Half} - 2 \quad \text{Half} - 1 \quad \text{Half}
 \end{array}$$

For case 6, when  $N$  is odd,  $N - 1$  is divisible by 4 but  
 $N - 1$  is not divisible by 8:

Half = (N + 1)/2  
 Fourth = (N - 1)/4

$$\text{Num}^{1/4} = \begin{bmatrix} -1 & 2 & -1 & 0 & \dots & & & & & \\ & 0 & -2 & 0 & 0 & \dots & & & & \\ & & & 2 & 0 & -1 & 0 & \dots & & \\ & & & & 0 & 0 & 0 & 0 & \dots & \\ & & & & & 0 & 0 & 1 & 0 & \dots \\ & & & & & & -1 & 0 & 0 & 0 & \dots \\ & & & & & & & \dots & \dots & \dots & \dots \\ & & & & & & & & 0 & 0 & 2 & -2 & \dots \\ & & & & & & & & & 2 & -2 & 0 & 2 & \dots \\ & & & & & & & & & & 0 & 2 & 0 & 0 & \dots \\ & & & & & & & & & & & 0 & 0 & -1 & 0 & \dots \\ & & & & & & & & & & & & 1 & 0 & 0 & \dots \\ & & & & & & & & & & & & & \dots & \dots & \dots & \dots \\ & & & & & & & & & & & & & & 1 & -2 & 0 \\ & & & & & & & & & & & & & & & 1 & 0 \\ & & & & & & & & & & & & & & & & 0 \end{bmatrix} \begin{array}{l} \text{Row :} \\ 1 \\ 2 \\ 3 \\ 4 \\ \text{Repeat} \\ \text{Repeat} \\ \dots \\ \text{Fourth} \\ \text{Fourth} + 1 \\ \text{Fourth} + 2 \\ \text{Repeat} \\ \text{Repeat} \\ \dots \\ \text{Half} - 2 \\ \text{Half} - 1 \\ \text{Half} \end{array} \tag{28}$$

$$\text{Dem}^{1/2} = \begin{bmatrix} -1 & 1 & 0 & -1 & 0 & 0 & \dots & 0 & 0 & 2 \end{bmatrix}$$

Col : 1 2 3 4 5 6 ... Half - 2 Half - 1 Half

For case 7, when N is odd, N + 1 is divisible by 4 and N + 1 is divisible by 8:

Half = (N + 1)/2  
 Fourth = (N + 1)/4

$$\text{Num}^{1/4} = \begin{bmatrix} -1 & -2 & 0 & 1 & 0 & \dots & & & & & \\ & 1 & 1 & -1 & 0 & 0 & \dots & & & & \\ & & 0 & 0 & 0 & 0 & \dots & & & & \\ & & & 0 & 0 & -1 & 0 & \dots & & & \\ & & & & 1 & 0 & 0 & 0 & \dots & & \\ & & & & & 0 & 0 & 1 & 0 & \dots & \\ & & & & & & -1 & 0 & 0 & 0 & \dots \\ & & & & & & & -1 & 0 & 2 & 0 & \dots \\ & & & & & & & & 0 & 2 & 2 & -2 & 0 & \dots \\ & & & & & & & & & 2 & -2 & 0 & 0 & \dots \\ & & & & & & & & & & 0 & 0 & -1 & 0 & \dots \\ & & & & & & & & & & & 1 & 0 & 0 & \dots \\ & & & & & & & & & & & & \dots & \dots & \dots & \dots \\ & & & & & & & & & & & & & 0 & 1 & 0 \\ & & & & & & & & & & & & & & 1 & 0 \\ & & & & & & & & & & & & & & & 0 \end{bmatrix} \begin{array}{l} \text{Row :} \\ 1 \\ 2 \\ 3 \\ 4 \\ 5 \\ \text{Repeat} \\ \text{Repeat} \\ \text{Fourth} - 1 \\ \text{Fourth} \\ \text{Fourth} + 1 \\ \text{Repeat} \\ \text{Repeat} \\ \dots \\ \text{Half} - 2 \\ \text{Half} - 1 \\ \text{Half} \end{array} \tag{29}$$

$$\text{Dem}^{1/2} = \begin{bmatrix} -1 & -1 & 1 & 0 & 0 & 0 & \dots & 0 & 0 & 2 \end{bmatrix}$$

Col : 1 2 3 4 5 6 ... Half - 2 Half - 1 Half

For case 8, when N is odd, N + 1 is divisible by 4 but N + 1 is not divisible by 8:

Half = (N + 1)/2  
 Fourth = (N + 1)/4

$$\begin{array}{l}
 \text{Num}^{1/4} = \begin{bmatrix} -1 & -2 & 0 & 0 & 0 & \dots \\ & 1 & 2 & -1 & 0 & 0 & \dots \\ & & 0 & 0 & -1 & 0 & \dots \\ & & & 1 & 0 & 0 & 0 & \dots \\ & & & & 0 & 0 & 1 & 0 & \dots \\ & & & & & -1 & 0 & 0 & 0 & \dots \\ & & & & & & \dots & \dots & \dots & \dots \\ & & & & & & & -1 & 0 & 2 & 0 & \dots \\ & & & & & & & 0 & 2 & 2 & -2 & 0 & \dots \\ & & & & & & & & 2 & -2 & 0 & 0 & \dots \\ & & & & & & & & & 0 & 0 & -1 & 0 & \dots \\ & & & & & & & & & & 1 & 0 & 0 & \dots \\ & & & & & & & & & & \dots & \dots & \dots & \dots \\ & & & & & & & & & & & 1 & 0 & \text{Half} - 1 \\ & & & & & & & & & & & 0 & \text{Half} \end{bmatrix} \\
 \text{Dem}^{1/2} = \begin{bmatrix} -1 & -1 & 1 & 0 & 0 & 0 & \dots & 0 & 0 & 2 \end{bmatrix} \\
 \text{Col} : 1 & 2 & 3 & 4 & 5 & 6 & \dots & \text{Half} - 2 & \text{Half} - 1 & \text{Half}
 \end{array}
 \tag{30}$$

As the new formulas were developed from the algorithms, numerical calculation, instead of analytical demonstrations of trigonometric relations, is necessary to check them. It is believed that a large number of numerical tests can validate or verify these new formulas, or at least reduce the chance of these formulas being wrong or false, to a minimum. The goal here is to verify that the new formulas really calculate the tangent of the phase [tan(φ)]. For that, real figures are attributed to random  $I_m$  that ranges from 0 to 128 that are assigned at random to real values,  $I_a$  that ranges from 0 to 127, and the cosine of -1 varies by 1 to the values of luminous intensity  $I_k$  will be between 0 and 255 that is the range of values of pixels obtained in monochrome digital photographs. It is interesting to note that the digital images and values are intact here to further enlarge the test in which they are made real. They are also assigned values to real random  $\phi'$  that varies from  $-\pi$  to  $\pi$ , tracking common algorithms used on the main unwrapped. Real values are assigned and the random  $\delta$  that ranges from  $-10\pi$  to  $10\pi$ , a very wide range of possible values of step phase. The values of  $I_k$  (luminous intensity of the image) are calculated, with  $k$  ranging from 1 to  $N$ . The new formulas with the values of  $I_k$  are applied, giving a tan(φ) that must be compared with the value of phase randomly assigned

(φ''). This comparison is the accuracy through a very small  $n$  because the number of rounding errors that can occur in the calculations, say, precision  $|\phi' - \phi| \leq 10^{-6}$ . This was done thousands of times (at least 10 000 times) for each formula for phase calculation. It generated and made up of at least 99.9% of the time with an accuracy of  $10^{-6}$ . Thus, it was believed that the chances for the formulas to be wrong or false have become minimal or remote.

**Before Unwrapping, Change  $\phi \in [0, \pi/2]$  to  $\phi^* \in [-\pi, \pi]$**

Because of the character of the evaluation algorithms, only phase values  $\phi \in [0, \pi/2]$  were calculated. For unequivocal determination of the wrapped phase values  $\phi$  it was necessary to test four values  $\phi, -\phi, \phi - \pi$  and  $-\phi + \pi$  using values of  $I_k$  and small systems. With this, the value  $\phi^* \in [-\pi, \pi]$  was obtained [3–6]. In case  $N = 5$ , with  $I_1, I_2, I_3, I_4$  and  $I_5$ ,  $\delta$  was found in the first equation and the values  $\phi, -\phi, \phi - \pi$  and  $-\phi + \pi$  were attributed to  $\phi^*$  to test the other equation and  $I_a$  was found using a second equation. As an example, for each (x, y) it was tested for the four values  $\phi, -\phi, \phi - \pi$  and  $-\phi + \pi$  in (addition and subtraction of first, last and middle frames, the  $I_k$ ):

$$\text{even } N = 4 \begin{cases} \cos(\delta/2) = \pm \sqrt{\frac{I_1 - I_4}{4(I_2 - I_3)}} \\ I_1 - I_4 = 2I_a \sin(\phi^*) \sin(3\delta/2) \\ I_2 - I_3 = 2I_a \sin(\phi^*) \sin(\delta/2) \\ (I_1 + I_4) - (I_2 + I_3) = 2I_a \cos(\phi^*) [\cos(3\delta/2) - \cos(\delta/2)] \\ I_1 - I_3 = I_a [\cos(\phi^* - 3\delta/2) - \cos(\phi^* + \delta/2)] \end{cases}
 \tag{31}$$

$$\text{odd } N = 5 \begin{cases} \cos(\delta) = \frac{I_1 - I_5}{2(I_2 - I_4)} \\ I_1 - I_5 = 2I_a \sin(\phi^*) \sin(2\delta) \\ I_2 - I_4 = 2I_a \sin(\phi^*) \sin(\delta) \\ I_1 + I_5 - 2I_3 = 2I_a \cos(\phi^*) [\cos(2\delta) - 1] \\ I_2 + I_4 - 2I_3 = 2I_a \cos(\phi^*) [\cos(\delta) - 1]. \end{cases} \quad (32)$$

In a different approach, for unambiguous determination of the wrapped phase values, it is necessary to test four values  $\phi$ ,  $-\phi$ ,  $\phi - \pi$  and  $-\phi + \pi$  using values of  $I_k$  and to solve small nonlinear systems (Newton–Raphson methods). For each angle  $\phi$ ,  $-\phi$ ,  $\phi - \pi$  and  $-\phi + \pi$ , solve the nonlinear system by Newton–Raphson in Equation (25), getting the values of  $I_m$ ,  $I_a$  and  $\delta$ .

$$\begin{cases} I_1 - (I_m + I_a \cos[\phi * + (\frac{2 \cdot 1 - N - 1}{2}) \delta]) = 0 \\ I_2 - (I_m + I_a \cos[\phi * + (\frac{2 \cdot 2 - N - 1}{2}) \delta]) = 0 \\ I_3 - (I_m + I_a \cos[\phi * + (\frac{2 \cdot 3 - N - 1}{2}) \delta]) = 0 \end{cases} \quad (33)$$

With the values of  $I_m$ ,  $I_a$  and  $\delta$ , test the Equation (36) and find the correct angle  $\phi^* \in [-\pi, \pi]$ .

$$\begin{cases} I_4 - (I_m + I_a \cos[\phi * + (\frac{2 \cdot 4 - N - 1}{2}) \delta]) = 0 \\ \dots \\ I_N - (I_m + I_a \cos[\phi * + (\frac{2N - N - 1}{2}) \delta]) = 0 \end{cases} \quad (34)$$

### Testing and Analysis of Error

The phase  $\phi^*$  obtained from the phase-shifting algorithm above is a wrapped phase, which varies from  $-\pi/2$  to  $\pi/2$ . The relationship between the wrapped phase and the unwrapped phase may thus be stated as:

$$\Psi(x, y) = \phi^*(x, y) + 2\pi j(x, y) \quad (35)$$

where  $j$  is an integer number,  $\phi^*$  is a wrapped phase and  $\psi$  is an unwrapped phase.

The next step is to unwrap the wrapped phase map [10]. When unwrapping, several of the phase values should be shifted by an integer multiple of  $2\pi$ . Unwrapping is thus adding or subtracting  $2\pi$  offsets at each discontinuity encountered in phase data. The unwrapping procedure consists of finding the correct field number for each phase measurement [11–13].

The modulation phase  $\psi$  obtained by unwrapping physically represents the fractional fringe order numbers in the Moire images. The shape can be determined by applying the out-of-plane deformation equation for shadow Moire:

$$Z(x, y) = \frac{p[\Psi(x, y)/2\pi]}{(\tan \alpha + \tan \beta)} \quad (36)$$

where  $Z(x, y)$  = elevation difference between two points located at body surface to be analysed;  $p$  = frame period;  $\alpha$  = light angle;  $\beta$  = observation angle.

The experiments were carried out using square wave grating with 1-mm frame grid period; the light source is the common white of 300 W without using plane waves; light angle ( $\alpha$ ) and observation angle ( $\beta$ ) are  $45^\circ$ ; the object surface is white and smooth and the resolution of photograph is 1 megapixel. Phase stepping is made by displacing the grid in the horizontal direction in fractions of millimetres (Figure 3).

To test the new algorithms for phase calculation, they were used with the technique of shadow Moire [14] for an object with known dimensions and to evaluate the average error by Equation (37). This process was started with four images, repeated with five, then six and so on. The idea was to show that with increasing number of images the average error tends to decrease. Figure 4 shows this procedure.

$$\text{Error Median}(E) = \frac{1}{M} \sum_{i=1}^M |Z_i^e - Z_i| \quad (37)$$

where  $M$  is the number of pixels of the image,  $Z_i^e$  is the exact value of the size of the object being measured and  $Z_i$  is value measured by the new algorithm.

To compare the new algorithms for calculating the phase, 21 sets of 16 photographs each were selected. Each set was computed using the average error of 4 to 16 images and using algorithms to evaluate the number of images. An average of errors was estimated, then 21 sets were evaluated using 4 to 16 images in each set ( $\mu_4, \mu_5, \mu_6, \dots, \mu_{16}$ ). The hypothesis of testing on the difference in the means  $\mu_A - \mu_B$  of two normal populations is being considered at the moment. A more powerful experimental procedure is to collect the data in pairs – that is, to make two hardness readings on each specimen, one with each tip. The test procedure would then consist of analy-

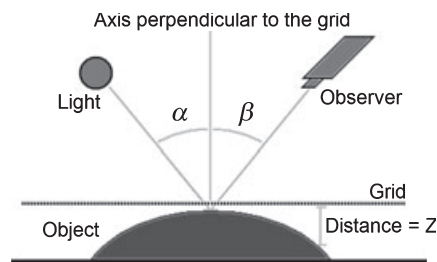
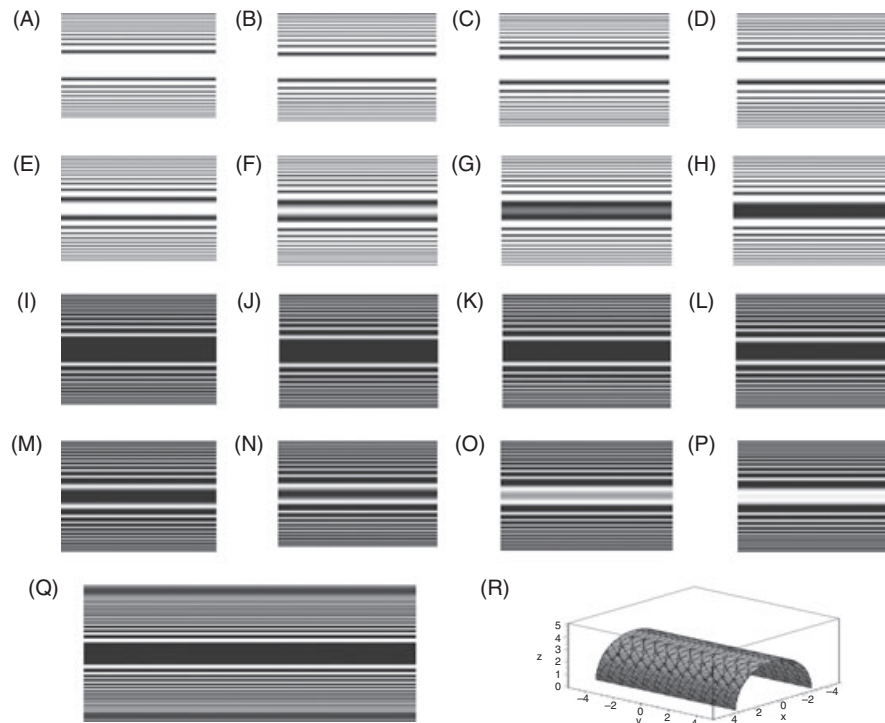


Figure 3: Layout of experiment



**Figure 4:** One set of photographs of 1 megabyte. Original shadow Moiré images; 16-frame phase-shifting algorithm [A-P]. Wrapped phase [Q]. Result in 3D [R] (Semi-cylinder of a motor with diameter 6 cm, length 12 cm and with frame period of grid 1 mm.)

**Table 4:** Error median error in  $\mu\text{m}$  versus number of frames ( $N$ ) for semi-cylinder with diameter of 6 cm and length of 12 cm (frame period of grid with 1 mm). It used 21 different sets of 16 images of shadow Moiré (Figure 4)

Error median ( $\mu\text{m}$ )		Sets of images																				
No. images	Equation	1	2	3	4	5	6	7	8	9	10	11	12	13	14	15	16	17	18	19	20	21
4	a	126	127	126	126	127	129	129	127	129	127	129	127	127	128	127	126	128	126	126	125	127
	b	124	122	123	122	124	123	124	121	124	121	124	122	125	125	122	123	124	122	124	122	122
6	a	120	117	119	119	119	118	118	119	117	117	119	121	119	120	120	117	120	120	118	120	119
	b	118	119	117	119	120	117	119	117	118	117	119	118	119	120	119	118	117	119	118	119	120
	c	119	120	119	119	120	118	117	118	118	117	117	119	120	120	120	119	120	121	118	118	117
	d	118	119	120	118	118	120	118	121	118	120	117	120	120	120	118	117	118	120	117	118	118
	e	120	118	117	117	119	119	118	117	118	117	117	120	119	121	120	117	117	118	121	117	120
7	a	115	115	114	113	116	115	114	115	115	116	113	116	113	113	116	113	116	114	114	115	115
	b	116	114	115	114	116	114	113	115	116	116	113	115	116	117	116	116	116	113	116	115	115
	c	113	114	114	114	115	113	116	113	116	113	116	113	116	114	116	116	115	116	114	116	113
	d	115	115	116	116	114	113	115	113	117	113	114	117	114	115	114	113	114	114	113	115	114
8	a	109	110	110	109	110	112	112	111	110	110	109	112	110	112	110	111	109	109	112	108	108
	b	110	112	111	112	111	112	112	109	110	110	110	109	110	110	110	108	112	110	110	109	109
	c	112	110	111	112	111	112	110	108	110	111	109	110	110	111	111	111	112	112	109	110	109
	d	111	109	111	109	110	111	111	109	110	110	109	110	112	110	112	109	109	110	110	109	112
9	a	106	107	105	105	105	106	105	108	108	105	105	108	107	106	105	105	104	105	106	108	108
	b	108	108	106	108	106	107	105	106	107	108	107	107	105	105	104	105	107	105	105	105	106
	c	105	108	108	104	105	104	106	105	105	106	107	106	106	105	105	108	108	105	108	106	106
10	a	100	101	100	101	103	101	104	101	103	103	104	102	102	102	101	101	103	101	100	103	103
	b	103	102	103	101	100	103	102	102	103	101	102	101	102	103	100	103	100	102	104	102	103
	c	104	102	102	103	100	104	102	102	101	104	103	100	102	102	100	104	100	103	100	101	102
11	a	97	99	99	99	97	97	96	99	97	96	99	98	98	98	98	100	97	98	98	98	96
	b	97	99	97	97	98	98	100	99	100	97	96	98	97	97	97	97	97	98	97	98	98
	c	97	99	98	98	97	96	97	97	96	97	97	99	98	97	96	97	99	99	97	99	100
12	a	95	93	96	94	94	94	92	93	95	93	94	94	96	93	94	95	96	94	93	92	92
	b	93	92	92	94	96	92	95	93	94	93	95	92	96	93	96	92	93	93	95	94	95

**Table 4:** (Continued)

Error median ( $\mu\text{m}$ )		Sets of images																				
No. images	Equation	1	2	3	4	5	6	7	8	9	10	11	12	13	14	15	16	17	18	19	20	21
13	a	92	92	91	88	90	89	88	91	90	88	89	89	88	90	90	88	88	90	90	88	91
	b	88	91	91	88	90	88	88	91	89	90	89	88	91	88	89	90	91	92	91	90	91
14	a	85	87	83	85	87	84	86	86	84	86	84	84	84	86	85	86	84	84	86	84	87
	b	87	85	87	86	87	87	85	85	87	86	86	85	86	83	84	85	87	85	84	87	86
15	a	83	82	82	82	84	83	85	85	83	85	82	82	82	82	83	85	85	83	81	84	84
16	a	80	78	78	80	79	80	79	80	81	79	80	78	77	78	79	80	79	79	79	78	81

**Table 5:** Testing hypotheses about the difference between two means with paired *t*-test,  $H_0: \mu_A - \mu_B = 0$  against  $H_1: \mu_A - \mu_B \neq 0$ . The *P*-value is the smallest level of significance that would lead to rejection of the null hypothesis  $H_0$  with the given data

P-value	No. images and formula																													
		4	5	6	7			8			9			10		11		12		13		14		15						
		a	a	a	b	c	d	e	a	b	c	d	a	b	c	d	a	b	c	a	b	c	a	b	c	a	b	a	b	a
4	a																													
5	a 0%																													
6	a 0% 0%																													
	b 0% 0% 17%																													
	c 0% 0% 49% 55%																													
	d 0% 0% 52% 57% 98%																													
	e 0% 0% 20% 85% 49% 53%																													
7	a 0% 0% 0% 0% 0% 0%																													
	b 0% 0% 0% 0% 0% 0% 10%																													
	c 0% 0% 0% 0% 0% 0% 95% 17%																													
	d 0% 0% 0% 0% 0% 0% 85% 13% 79%																													
8	a 0% 0% 0% 0% 0% 0% 0% 0%																													
	b 0% 0% 0% 0% 0% 0% 0% 0% 81%																													
	c 0% 0% 0% 0% 0% 0% 0% 0% 45% 51%																													
	d 0% 0% 0% 0% 0% 0% 0% 0% 98% 78% 34%																													
9	a 0% 0% 0% 0% 0% 0% 0% 0% 0% 0%																													
	b 0% 0% 0% 0% 0% 0% 0% 0% 0% 0% 81%																													
	c 0% 0% 0% 0% 0% 0% 0% 0% 0% 0% 100% 82%																													
10	a 0% 0% 0% 0% 0% 0% 0% 0% 0% 0% 0% 0%																													
	b 0% 0% 0% 0% 0% 0% 0% 0% 0% 0% 0% 0% 77%																													
	c 0% 0% 0% 0% 0% 0% 0% 0% 0% 0% 0% 0% 75% 97%																													
11	a 0% 0% 0% 0% 0% 0% 0% 0% 0% 0% 0% 0%																													
	b 0% 0% 0% 0% 0% 0% 0% 0% 0% 0% 0% 0% 0% 77%																													
	c 0% 0% 0% 0% 0% 0% 0% 0% 0% 0% 0% 0% 0% 55% 83%																													
12	a 0% 0% 0% 0% 0% 0% 0% 0% 0% 0% 0% 0%																													
	b 0% 0% 0% 0% 0% 0% 0% 0% 0% 0% 0% 0% 0% 0% 46%																													
13	a 0% 0% 0% 0% 0% 0% 0% 0% 0% 0% 0% 0%																													
	b 0% 0% 0% 0% 0% 0% 0% 0% 0% 0% 0% 0% 0% 0% 61%																													
14	a 0% 0% 0% 0% 0% 0% 0% 0% 0% 0% 0% 0%																													
	b 0% 0% 0% 0% 0% 0% 0% 0% 0% 0% 0% 0% 0% 0% 15%																													
15	a 0% 0% 0% 0% 0% 0% 0% 0% 0% 0% 0% 0%																													
16	a 0% 0% 0% 0% 0% 0% 0% 0% 0% 0% 0% 0%																													



sing the differences between the hardness readings on each specimen. If there is no difference between tips, the mean of the differences should be zero. This test procedure is called the paired  $t$ -test [10]. Specifically, testing  $H_0: \mu_A - \mu_B = 0$  against  $H_1: \mu_A - \mu_B \neq 0$ . Test statistics is  $t_0 = D/(S_D/\sqrt{21})$  where  $D$  is the sample average of the differences and  $S_D$  is the sample standard deviation of these differences. The rejection region is  $t_0 > t_{\alpha/2,20}$  or  $t_0 < -t_{\alpha/2,20}$ . The data are shown in Table 4.

On performing the statistical test ( $H_0: \mu_A - \mu_B = 0$  against  $H_1: \mu_A - \mu_B \neq 0$ ) it was noticed that one cannot reject the zero hypothesis when using different algorithms with the same number of images. Furthermore, the null hypothesis can be rejected when using different algorithms with different number of images with level of significance ( $\alpha = 0.05$ ). It was concluded that the algorithms for phase calculation with a greater number of images are more accurate than those with smaller number of images. The tests are shown in Table 5.

## Conclusions

This paper deals with the algorithms for phase calculation in measurement with images method using the phase shifting technique. It describes several multistep phase-shifting algorithms with the constant, but unknown phase step between the captured intensity frames. The new algorithms are shown to be capable of processing the optical signal of Moiré images. These techniques are very precise, easy to use, and have a small cost. The results show that new algorithms were precise and accurate. On the basis of the performed error analysis it can be concluded that the new algorithms are very good phase calculation algorithms. These algorithms also seem to be a very accurate and stable phase shifting algorithms with the unknown phase step for a wide range of phase-step values. The metric analysis of the considered system demonstrated that its uncertainties of measurement depend on the frame period of the grid, of the resolution of photographs in pixel and of the number of frames. However, the uncertainties of measurement of the geometric parameters and the phase still require attention. In theory, if we have many frames, the measurement errors become very small. The measurement results

obtained by the optical system demonstrate its industrial and engineering applications in experimental strain analysis.

## ACKNOWLEDGEMENTS

The authors thank the generous support of the Pontificia Universidade Catolica de Minas Gerais – PUCMINAS, as well as of the Conselho Nacional de Desenvolvimento Científico e Tecnológico – CNPq – ‘National Counsel of Technological and Scientific Development’.

## REFERENCES

- Schreiber, H. and Bruning, J. H. (2007) Phase shifting interferometry. In: *Optical Shop Testing* (D. Malacara Ed.), Wiley Interscience, New York: 547.
- Malacara, D., Servín M. and Malacara, Z. (2005) *Interferogram Analysis for Optical Testing*. Taylor & Francis, New York: 414.
- Huang, P. S. and Guo, H. (2008) Phase-shifting Shadow Moiré Using the Carré Algorithm. *Proceedings of the SPIE*, San Diegop 7066, 70660B–70667B.
- Novak J. (2003) Five-step phase-shifting algorithms with unknown values of phase shift. *Int. J. Light Electron Optics Optik* 114, 63–68.
- Novak, J., Novak, P. and Miks, A. (2008) Multi-step phase-shifting algorithms insensitive to linear phase shift errors. *Optics Commun.* 281, 5302–5309.
- Creath, K. (1988) Phase measurement interferometry techniques. In: *Progress in Optics*, Vol. XXVI (E. Wolf, Ed.). Elsevier Science, Amsterdam: 349–393.
- Malacara, D. (Ed.). (1992) *Optical Shop Testing*. John Wiley and Sons, New York.
- Hillier, F. S. and Lieberman, G. J. (2005) *Introduction to Operations Research*. 8th edn [S.I.]: McGraw-Hill, New York.
- Cordero, R. R., Molimard, J., Martinez, A. and Labbe, F. (2007) Uncertainty analysis of temporal phase-stepping algorithms for interferometry. *Optics Commun.* 275, 144–155.
- Triola M. F. (c2007) *Elementary Statistics*, 10th edn. Addison Wesley, Boston.
- Ghiglia, D. C. and Pritt, M. D. (1998) *Two-dimensional Phase Unwrapping: Theory, Algorithms and Software*. John Wiley & Sons, Inc., New York.
- Huntley, J. M. (1989) Noise immune phase unwrapping algorithm. *Appl. Opt.* 28, 3268–3270.
- Zappa, E. and Busca, G. (2008) Comparison of eight unwrapping algorithms applied to Fourier-transform profilometry. *Optics Lasers Eng.* 46, 106–116.
- Han, C. and Han, B. (2006) Error analysis of the phase-shifting technique when applied to shadow moiré. *Appl. Opt.* 45, 1124–1133.